OPEN ACCESS
JOURNAL OF ADVANCED DIELECTRICS
Vol. 14, No. 1 (2024) 2245002 (9 pages)

DOI: 10.1142/S2010135X22450023

Investigation of electrophysical, photo- and gas-sensitive properties of $ZnO–SnO_2$ sol–gel films

Irina A. Gulyaeva[*,¶], Alexandra P. Ivanisheva[*], Maria G. Volkova[†], Victoria Yu. Storozhenko[†], Soslan A. Khubezhov[‡,§], Ekaterina M. Bayan[†] and Victor V. Petrov[*]

[*]*Research and Education Centre "Microsystem Technics and Multisensory Monitoring Systems" Southern Federal University, Russia*

[†]*Department of Chemistry, Southern Federal University, Russia*

[‡]*Department of Physics, North-Ossetian State University, 362025 Vladikavkaz, Russia*

[§]*Department of Physics and Engineering, ITMO University, 191002 Petersburg, Russia*

[¶]tenirka@mail.ru

Received 27 June 2022; Revised 27 September 2022; Accepted 1 February 2023; Published 23 February 2023

Thin nanocomposite films based on tin dioxide with a low content of zinc oxide (0.5–5 mol.%) were obtained by the sol–gel method. The synthesized films are 300–600 nm thick and contains pore sizes of 19–29 nm. The resulting $ZnO–SnO_2$ films were comprehensively studied by atomic force and Kelvin probe force microscopy, X-ray diffraction, scanning electron microscopy, and high-resolution X-ray photoelectron spectroscopy spectra. The photoconductivity parameters on exposure to light with a wavelength of 470 nm were also studied. The study of the photosensitivity kinetics of $ZnO–SnO_2$ films showed that the film with the Zn:Sn ratio equal to 0.5:99.5 has the minimum value of the charge carrier generation time constant. Measurements of the activation energy of the conductivity, potential barrier, and surface potential of $ZnO–SnO_2$ films showed that these parameters have maxima at ZnO concentrations of 0.5 mol.% and 1 mol.%. Films with 1 mol.% ZnO exhibit high response values when exposed to 5–50 ppm of nitrogen dioxide at operating temperatures of 200°C and 250°C.

Keywords: Sol–gel method, $ZnO–SnO_2$ films; gas-sensitive properties; surface potential; potential barrier; conduction activation energy.

1. Introduction

Recently, there has been a strong demand for the development of reliable, accurate and economical gas sensors with increased sensitivity, selectivity, and response time for the detection of harmful gases. Much attention is paid to gas sensors based on metal oxide. To improve the functional characteristics of gas sensors, gas-sensitive materials based on binary oxide systems are used, such as $ZnO:SnO_2$, $ZnO:In_2O_3$, $SnO_2:In_2O_3$, and $TiO_2:In_2O_3$.[1–3] Zinc oxide (ZnO) and tin dioxide (SnO_2) are the most applicable functional materials due to their excellent electrical and optical properties. SnO_2 has proven to be a highly sensitive material for detecting both reducing and oxidizing gases.[4] Many studies have shown the effective use of zinc oxide as an additive to tin dioxide to increase the sensitivity of a gas sensor. The band gap for ZnO is 3.37 eV, and for SnO_2 it is 3.6–3.8 eV.[5] For both materials, the nature of the n-type conductivity is determined by oxygen vacancies.[6–8] ZnO and SnO_2 can be advantageously combined in various proportions to obtain $ZnO–SnO_2$ composites, which exhibit high transmittance in the visible light range and high electronic conductivity.[9,10]

It is also known that even amorphous thin $ZnO–SnO_2$ films have a relatively high electron mobility.[11,12] Such films have good gas-sensitive characteristics. Thin films[13] of nanocomposite material based on ZnO with small additions (0.5–5 mol.%) of SnO_2 were obtained by solid-phase pyrolysis. It was shown that film with the composition Sn:Zn = 1:99 showed the best sensitivity at 200°C, since it had the highest concentration of oxygen vacancies, which contributed to a better occurrence of surface reactions. The synthesis of thin $SnO_2–ZnO$ films using the methods of organometallic chemistry is described in Ref. 14.

It is known that the sol–gel method for obtaining nanocomposite films has advantages over vacuum technologies, primarily due to the absence of the expensive equipment. When using this method, more flexible regulation of the element molar ratio becomes possible. The sol–gel method makes it possible to form oxide films with complex compositions.[15,16] Thus, sol–gel[17] $SnO_2–ZnO$ films were synthesized at 500°C for 1 h. The particle size was 10 nm and 8 nm for pure SnO_2 and $SnO_2–ZnO$ composite, respectively. Sensors based on this $SnO_2–ZnO$ film showed a high response of

[¶]Corresponding author.

727 at an operating temperature of 70°C for 20 ppm NO_2 with an average response time of about 2 min. The high composite sensitivity is attributed to the grain size, which provides a higher surface-to-volume ratio, allowing more NO_2 gas molecules to react with the sensor surface.

It was shown[18] that the adsorption/desorption of gas and oxygen molecules make the main contribution to the change in the potential barrier between grains in the film. The value of the potential barrier increases at temperatures from 150°C to 250°C.

The gas-sensitive properties[19] of ZnO–SnO_2 sol–gel films with a Zn:Sn molar ratio of 0:100, 1:99, and 5:95 to nitrogen dioxide were studied. The authors have shown a correlation between the activation energy of conductivity (E_a), calculated from the temperature dependence of the conductivity of a gas-sensitive material, and the response of nitrogen dioxide sensors based on ZnO–SnO_2 sol–gel films. It is known that the surface properties of thin oxide nanocomposite films are also determined by energy barriers existing between crystallites in a film based on a mixture of tin and zinc oxides SnO_2–ZnO. In Ref. 13, the method of thermally stimulated conductivity measurements was used, which made it possible to determine the "effective" value of the energy barrier (φ_b). Measurements of the photoconductivity parameters of thin films formed on nontransparent substrates were shown previously.[20] A study of the response kinetics of SnO_2–ZnO nanocomposite films with different Sn:Zn molar ratios showed that a film with a Sn:Zn ratio of 50:50 has the minimum value of the photoconductivity relaxation time constant (τ). At the same time, SnO_2 films with a small addition of ZnO have lower values of τ than ZnO films with a small addition of SnO_2. The last circumstance indicates shorter lifetimes of charge carriers in films with a high content of SnO_2.

This work is a continuation of the previous studies and is aimed to study the correlations between the physicochemical, surface and gas-sensitive properties of ZnO–SnO_2 sol–gel thin films.

2. Methods and Materials

Tin (IV) chloride pentahydrate $SnCl_4 \cdot 5H_2O$, zinc nitrate hexahydrate $Zn(NO_3)_2 \cdot 6H_2O$, and isopropyl alcohol as a solvent were used to obtain thin ZnO–SnO_2 films. All reagents used were of analytical grade or the highest available purity and were purchased from ECROS, Russia. The required amounts of salt (Zn:Sn were 0:100, 0.5:99.5, 1:99 and 5:95 mol.%, respectively) were dissolved in isopropyl alcohol. Samples in the future will be identified in the text as 0ZnO, 0.5ZnO, 1ZnO and 5ZnO, respectively. The resulting solution was left for some time until the gel matured, after which it was applied by pouring three times onto pre-prepared substrates: soda-lime glass, silicon, and polycor. The substrates were cleaned by chemical methods: boiling was carried out with a solution of potassium dichromate $K_2Cr_2O_7$ and nitric acid HNO_3 for 10 min, after which the substrates were washed three times with distilled water and treated with alcohol. Each deposited layer was dried first at room temperature, then in the drying cabinet at a temperature of 120°C. The final heat treatment was carried out in a muffle furnace at a temperature of 550°C for two h. Cooling was carried out together with a muffle furnace in air, which made it possible to obtain homogeneous coatings without cracks. The obtained materials were studied by X-ray diffraction (XRD) analysis (diffractometer ARL X'TRA, Thermo ARL, Switzerland, with CuKα X-ray radiation) and scanning electron microscopy (SEM, instrument microscope EMXplus 10/12 Bruker, Germany). X-ray photoelectron spectroscopy (XPS) studies were carried out on a Thermo Scientific K-Alpha spectrometer with a source of Al k-α monochromatic rays with an energy of 1486.7 eV.

The surface topography, as well as the measurement of excitation of the external investigation, were carried out using the probe nanolaboratory Ntegra (NT-MDT SI, Russia). For this purpose, the atomic force microscopy (AFM) method was first investigated, and then Kelvin probe force microscopy (KPFM) method was carried out. Surface scanning, evaluation of measurements, and measurement of the outer films surface were carried out with a probe in the semi-contact mode. When testing in AFM and KPFM, NSG10/Pt cantilever with a reflective side and a constant force of 11.2 N/m (TipsNano, Estonia) is used.

Electrophysical and gas-sensitive studies were carried out on a stand for studying the electrophysical properties of gas sensors and gas-sensitive properties using a setup for the formation of gas mixtures "Microgaz-F" (Russia).[13] For this, V–Ni metal contacts were formed over the films.

Gas-sensitive properties are measured by exposure to 5–50 ppm nitrogen dioxide (NO_2) in synthetic material at operating temperatures of 100°C, 150°C and 250°C. Mixtures of air and NO_2 of a given concentration were formed using cylinders with calibration gas mixtures, injected at a flow rate of 0.3 dm^3/min. The response of sensor elements is calculated by the following equation:

$$S = R_g/R_0, \quad (1)$$

where R_0 is the sensor element in the absence of gas and R_g is the sensor element when exposed to gas.

The response (τ_{res}) and recovery (τ_{rec}) time were also evaluated. Using the stand, the temperature dependences of the electrical conductivity of the films were also measured. The method of measuring temperature-stimulated conductivity requires "effective" values of the energy barrier (φ_b).

To study the photoconductivity parameters of thin ZnO-SnO_2 films, a stand was developed and manufactured, the operation of which is based on measuring the photoconductivity kinetics of the film under study when it is irradiated with LED with a given wavelength. In addition, the design of the stand includes an AKIP-1101 (Russia) pulsed DC power supply, which allows one to adjust the energy characteristics of the radiation. To measure the characteristics of radiation, the CENTER 532 ultraviolet radiation intensity meter

(China) and the CENTER 530 illuminance meter (luxmeter) (China) are used. In this work, we studied the direct change in photoconductivity under the action of light from LED with a peak wavelength of 470 nm, which produces an illumination level of 525 lux on the sample. The measurements showed that the ultraviolet component was present in this case.

3. Results and Discussion

The composition and stoichiometry of the resulting oxide films were studied by XPS. In Table 1, the complete surface composition and the Zn:Sn ratio in the ZnO–SnO_2 sol–gel films are presented. XPS studies show Zn:Sn ratios 2–2.5 times higher compared to Zn:Sn ratios in precursors.

The results obtained are due to the peculiarity of the XPS method and indicate the nanocomposite structure of the films. In Fig. 1, the C1s (a), O1s (b), Sn3d (c), and Zn2p (d) high-resolution XPS series, respectively, are shown.

As can be seen from Fig. 1(a), the series of curves for C1s photoelectron lines are almost identical and correspond to adsorbed atmospheric carbon with bonds C–C (284.8 eV — red area), C–O (286 eV — green area) and C=O (288.6 eV — blue area), respectively. The change in the shape and position of the maxima of the O1s photoelectronic curves (Fig. 1(b)) indicates a change in the component composition in the samples; in particular, as zinc is added, the maximum of the O1s line shifts to lower energies, which is due to the formation of an oxide with a binding energy of ~529.6 eV.[21] For the best perception the areas corresponding to the bonds of oxygen with carbon, hydrogen and metals are highlighted in gray, green, red, and blue, respectively. The XPS spectra of tin (Fig. 1(c)) unambiguously correspond to tin (IV) oxide. The change in the shape of the lines as tin dioxide with zinc oxide is due to the partial overlap of the photoelectron Sn3d maxima with the Auger electron transitions of zinc.[22] Analysis of a series of photoelectron spectra of zinc (Fig. 1(d)) demonstrates a significant change in the position and shape of the curves with an increase of zinc oxide in the ZnO–SnO_2 sol–gel films. Thus, the maximum intensity of the Zn 2p3 doublet peak (Fig. 1(d), green area — 1) corresponds to 1021.5 eV, which is 0.2 eV higher than in the case of bulk zinc oxide. In addition, there is an intense peak of plasmon losses in the region 2 — gray color (Fig. 1(d)). The blue color in Fig. 1(d) (region 3) corresponds to the Auger electron transitions of Sn MN.[23] The presence of metallic states of zinc in oxide films is ruled out both by the shape of the Zn2p peak and by its position. But since the intensity of the peaks of zinc plasmonic losses in the region of 1033 eV (Fig. 1(d) 2-gray color) is commensurate with photoelectronic ones, this suggests a special reduced state of zinc in zinc oxide ZnO–SnO_2 sol–gel films. The last circumstance may be due to the presence of a strong surface electric field in thin nanocomposite films.[9]

The crystal structure of the synthesized materials was investigated using XRD analysis using CuKα XRD radiation at 35 kV and 30 mA. All the obtained film materials are nanosized, insufficiently crystallized, and contain the main phase of cassiterite. As the zinc content in the sample decreases, the degree of crystallinity and the intensity of the peaks decrease.

Table 1. Surface composition of ZnO–SnO_2 films.

	Surface composition, atomic %				Zn:Sn ratio, %	
Sample	C	O	Sn	Zn	Zn	Sn
0ZnO	45.5	27.5	27.0	0	0	100
0.5ZnO	45.7	26.9	26.9	0.4	1.4	98.6
1ZnO	45.1	27.5	26.7	0.7	2.5	97.5
5ZnO	44.7	25.4	27.1	2.8	9.9	90.1

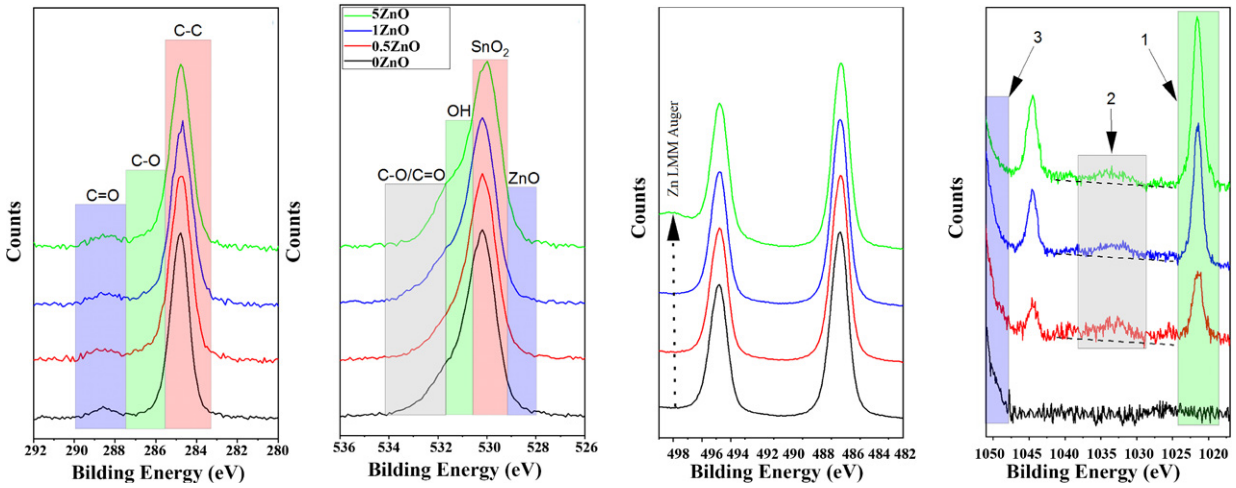

(a) (b) (c) (d)

Fig. 1. High-resolution XPS spectra C1s (a), O1s (b), Sn3d (c) and Zn2p (d) of ZnO–SnO_2 films (0ZnO, 0.5ZnO, 1ZnO, 5ZnO — black, red, blue, and green lines, respectively).

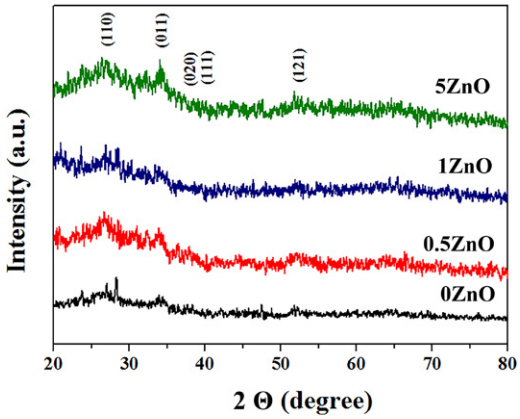

Fig. 2. XRD patterns of ZnO–SnO_2 films.

The lowest peak intensity is observed for the sample with the 0.5 mol.% Zn concentration.

XRD patterns of ZnO–SnO_2 films are presented in Fig. 2. According to XRD data, regardless of the ZnO concentration, all materials are nanosized, crystallized, and have a cassiterite structure.

The average crystallite size estimated from XRD data is 19–25 nm for sieved 0ZnO, 0.5ZnO, 1ZnO, and 5ZnO films. SEM images of 0ZnO, 0.5ZnO, 1ZnO and 5ZnO, respectively are presented in Fig. 3. Thus, the largest increase in pore size is observed for 1ZnO film. About 100–150 pores were selected for statistical analysis and the pore size was determined. The software Image J and Digimizer 4.1.1.0 are used to measure the sample porosity. The error of statistical analysis was ±3 nm. Statistical histograms were constructed based on the obtained data (Fig. 3). The thickness of the obtained films was 300–600 nm.

Analysis of porosity by SEM images showed that the average pore sizes of 0ZnO, 0.5ZnO, 1ZnO and 5ZnO films were 8, 27, 22, and 14 nm, respectively. From Fig. 3, it can be concluded that with the addition of ZnO, the average pore size increases. This is a well-known fact that is observed when adding salts of the second component to the precursor in sol–gel technology.[24–26]

The surface morphology of ZnO–SnO_2 films was studied by AFM, and the charge state of the surface by KPFM. Surface images of ZnO–SnO_2 films are shown in Fig. 4.

AFM studies have shown that films have a developed surface morphology. With an increase in the ZnO content, the root-mean-square roughness *Sq* decreases almost twice, from 6 nm to 3 nm, and the height difference *Sy* decreases more than twice, from 75.5 nm to 29.0 nm.

To estimate the activation energy of conductivity in thin nanocomposite SnO_2–ZnO films, the temperature dependences of the film's conductivity were measured in the range from room temperature to 300°C — Fig. 5.

The activation energy of conductivity was calculated. Analysis of the presented dependences shows that the

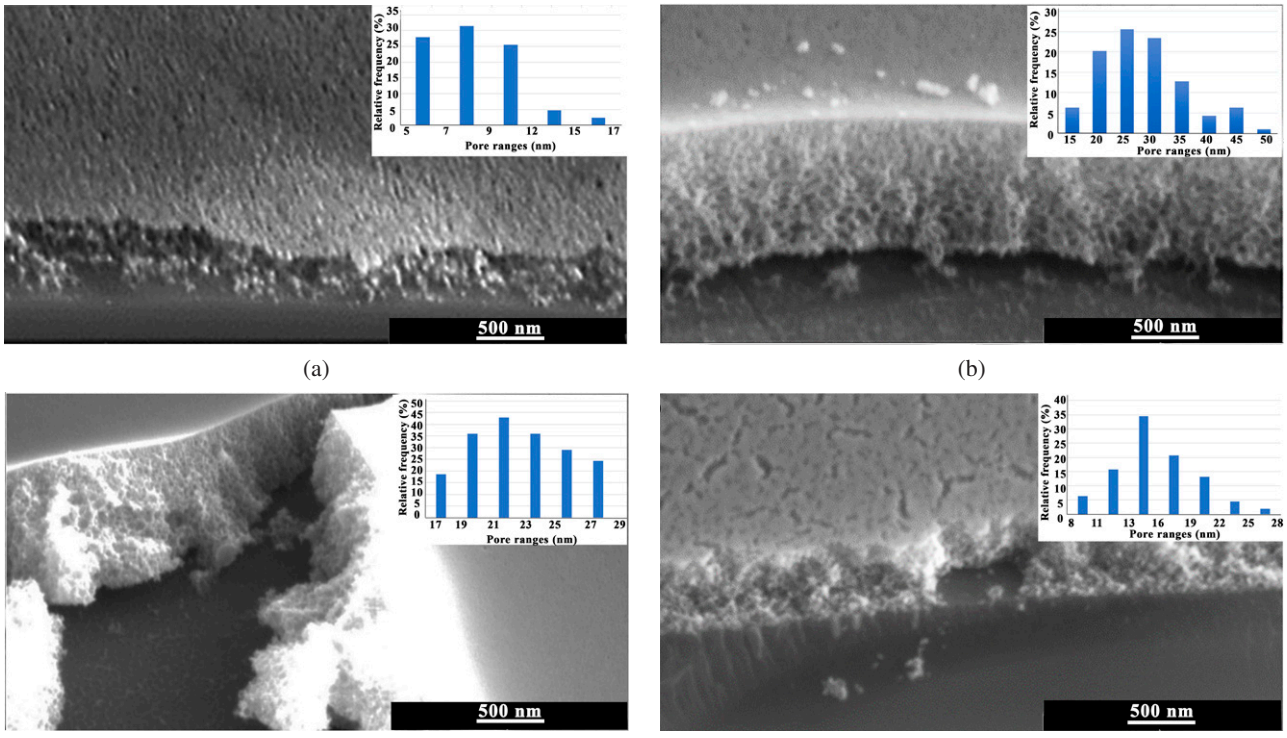

Fig. 3. Dependences of the films pore sizes on the relative frequency and SEM images of materials: (a) 0ZnO, (b) 0.5ZnO, (c) 1ZnO and (d) 5ZnO.

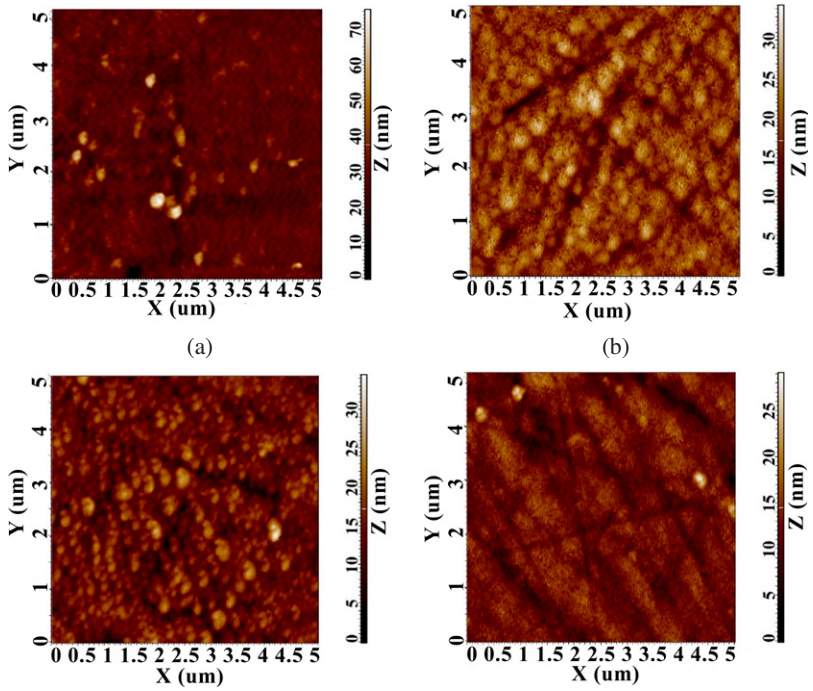

Fig. 4. AFM images of 0ZnO (a), 0.5ZnO (b), 1ZnO (c) and 5ZnO (d) films.

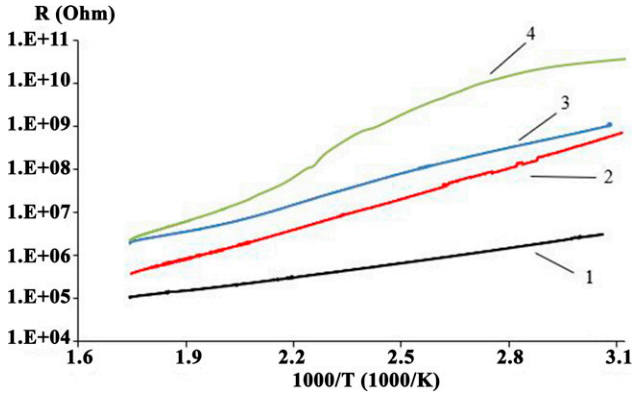

Fig. 5. Temperature dependence on resistance for 0ZnO (1), 0.5ZnO (2), 1ZnO (3) and 5ZnO (4) films.

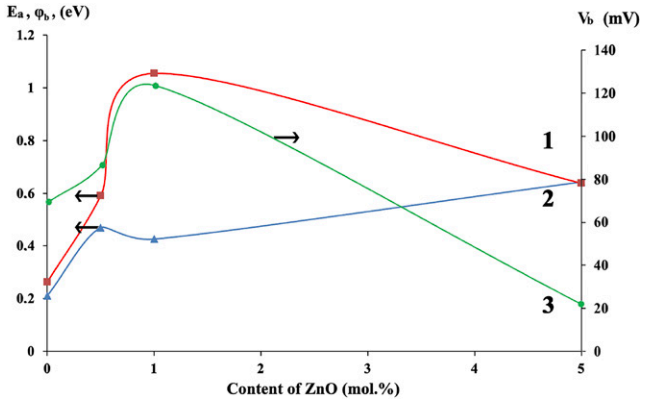

Fig. 6. Dependence of φ_b (1), E_a (2), and V_b (3) on the ZnO content in the film.

generation of charge carriers due to the thermal excitation is of an activation nature, that is, the dependence of the material resistivity on temperature is described by the Arrhenius equation[27] (Eq. (2)):

$$G = G_0 \cdot \exp^{(-Ea/k \cdot T)}, \quad (2)$$

where E_a is the activation energy of conductivity, k is the Boltzmann constant, and G_0 is the preexponential factor (const).

For 0ZnO, 0.5ZnO, 1ZnO and 5ZnO films, the activation energies of conductivity were 0.21, 0.47, 0.43 and 0.64, and potential barrier's values were 0.264, 0.59, 1.054 and 0.643, respectively. Figure 6 shows the dependence between the potential barrier, the activation energy, and the average values of the surface potential difference (V_b) on the ZnO content in the film.

Investigations by the KPFM method showed that the lowest average value of the surface potential, about 22 mV, is characteristic of the 5ZnO film (Fig. 6). The 0ZnO film has a low V_b value of 69 mV. The 1ZnO film has the highest value of V_b — 123.5 mV. The 0.5ZnO film also has a high surface potential equal to 86 mV. It is interesting that the last two films, according to XPS studies, have a special state of zinc oxide nanoclusters in the ZnO–SnO_2 sol–gel film, in which zinc can be in the reduced form.

Measurements of temperature-stimulated conductivity were important for the "effective" value of the energy barrier between the material grains of ZnO–SnO_2 nanocrystalline films. An analysis of the φ_b values showed that a maximum of 1.054 eV is observed for the 1ZnO film. Such values of activation energy and potential barrier, depending on the samples phase composition, can be associated with a change in defectiveness, grain boundary composition of tin dioxide and zinc oxide crystallites, and porosity of ZnO–SnO_2 nanocomposite films.

In this work, direct changes in photoconductivity were studied under the action of light from a LED with a peak wavelength of 470 nm. The measurements were carried out before the beginning of the "smoothing" of the dependencies. Subsequently, the time constant for the generation of charge carriers under the action of light was calculated — Fig. 7.

Studies have shown that pure tin dioxide has the highest time constant for the generation of charge carriers — 87 s. The addition of 0.5% and 5% zinc oxide to tin oxide drastically reduces the constant duration to 17–19 s. At the same time, with the addition of 1% zinc oxide, an increase in the time constant up to 43 s is observed.

This behavior of the photoconductivity parameters is associated with the nanocomposite structure of the film material, and lower values of the time constant are associated with a higher concentration of charge carrier generation centers at the ZnO–SnO_2 interface at a Sn:Zn ratio of 99.5:0.5. It can also be noted that the response kinetics for all films was similar, which indicates the same generation mechanisms — the recombination of charge carriers in SnO_2 sol–gel films with the addition of ZnO.

At temperatures up to 200°C, molecules of water and other gases are present on the surface of oxides,[28,29] which has a significant effect on gas-sensitive properties. Therefore, 150°C was chosen as the first temperature to study the effects associated with the influence of surface properties on gas-sensitive properties. Further, the temperature was increased by every 50°. It was found that at 200°C and 250°C the responses of the sensors are close, so the behavior of the films at higher temperatures was not studied. At the same time, it was shown that at an operating temperature of 150°C, as expected, the sensitivity to gases is significantly lower, which confirms previous studies.[19] In this case, a correlation is observed between the structure of the obtained materials and gas-sensitive properties. Thus, materials 0.5ZnO, 1ZnO have large pore sizes (Figs. 3(b) and 3(c)), which contributes to the active sorption of gases into materials. This leads to the fact that these materials are lower than the 0ZnO and 5ZnO materials (Figs. 3(a) and 3(d)), which have smaller pores.

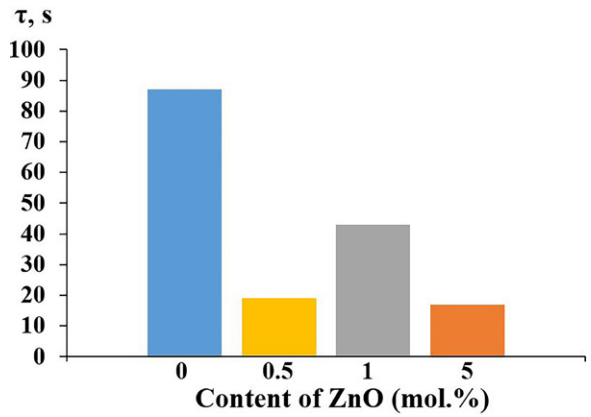

Fig. 7. Photoconductivity relaxation time constant of ZnO–SnO_2 films with different Zn:Sn ratios.

Figure 8(a) shows the responses of ZnO–SnO_2 samples of 0ZnO (1), 0.5ZnO (2), 1ZnO (3) and 5ZnO (4) to 50 ppm NO_2 at operating temperatures of 150°C, 200°C and 250°C. Figure 8(b) shows typical responses of ZnO–SnO_2 film samples to NO_2 at 50 ppm at 200°C. Figure 8(c) shows the concentration dependences of the 5ZnO response at different temperatures.

An increase in operating temperature from 150˚C to 250˚C leads to the response time decreasing from 620 s to 47 s. The recovery time also decreases from 297 s to 51 s at the same operating temperatures. For the 0ZnO, 0.5ZnO, 1ZnO, and 5ZnO samples τ_{res} is 155, 275, 512, and 101 s, and τ_{rec} is 160, 290, 600, and 110 s, respectively (Fig. 8(b)). The 5ZnO sample in the temperature range of 150˚C, 200˚C and 250˚C under the nitrogen dioxide exposure with a concentration of 50 ppm has the smallest response value τ_{res}, which is 204, 101 and 47 s, respectively, and τ_{rec} is equal to 220, 110 and 51 s.

In Ref. 19, a correlation was found between the conductivity activation energy E_a and the response of sensors based on ZnO–SnO_2 sol–gel films. The measurements of E_a, φ_b and V_b for ZnO–SnO_2 sol–gel films were provided, and the correlation of the sensor response when exposed to nitrogen dioxide with a concentration of 50 ppm at three operating temperatures of 150°C, 200°C and 250°C is shown in Figs. 6 and 8. The analysis of correlations was carried out in the Excel program using the maximum value of the correlation coefficient $R^2 > 0.95$, considering the exponential character dependence of the sensor response on E_a. At the same time, the dependence of the sensor response on φ_b and V_b may have a different character.

The analysis showed that at an operating temperature of 150°C, the response of the sensor based on ZnO–SnO_2 sol–gel films has a polynomial dependence on the surface potential V_b with a confidence factor R^2=0.99:

$$R_g/R_0 = 307.98 \cdot V_b^2 - 220.27\, V_b + 50.04. \quad (3)$$

It can be seen from Eq. (3) that the higher value of V_b corresponds to the higher response to the nitrogen dioxide. Measurements of V_b, KPFM method are carried out at room temperature. At the same time, at a temperature of 150°C, active desorption of water molecules does not occur on the oxide surface and there is approximately the same composition of molecules adsorbed from the atmosphere at room temperature. In this regard, at low operating temperatures,

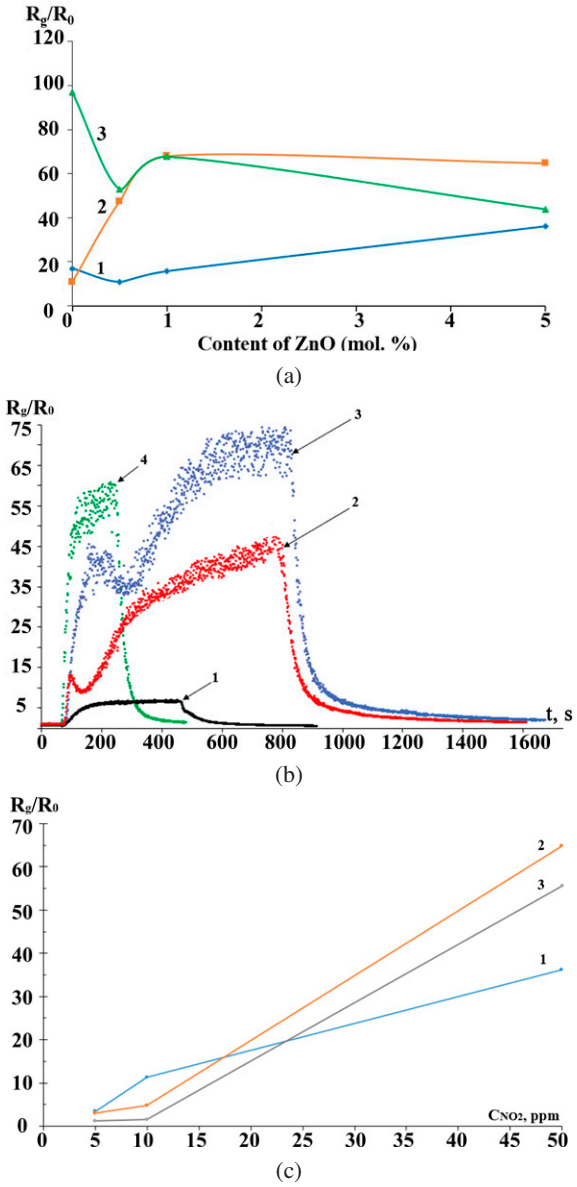

Fig. 8. (a) Response of ZnO–SnO_2 films to 50 ppm NO_2 at three operating temperatures 150°C (1), 200°C (2) and 250°C (3); (b) Typical responses of 0ZnO (1), 0.5ZnO (2), 1ZnO (3), and 5ZnO (4) film at 200°C; (c) Concentration dependences of the response of 5ZnO films at 150 °C (1), 200 °C (2) and 250°C (3).

the surface potential V_b will determine the response of the gas sensor: if the V_b increases, the sensor response value increases too.

At an operating temperature of 200°C, the response of a sensor based on ZnO–SnO_2 sol–gel films has a polynomial dependence on the potential barrier value ϕ_b with a confidence factor R^2=0.97:

$$R_g/R_0 = -119.97 \cdot \varphi_b{}^2 + 231.92\ \varphi_b - 42.64. \quad (4)$$

In contrast to the positive effect of the surface potential, the potential barrier makes rather the opposite contribution to the magnitude of the response. It can be seen from Eq. (4) that the higher φ_b corresponds to the smaller response to the nitrogen dioxide.

At an operating temperature of 250°C, the response of a sensor based on ZnO–SnO_2 sol–gel films has an exponential dependence on the activation energy of conductivity E_a with a confidence factor R^2=0.96:

$$R_g/R_0 = 142.54 \cdot e^{-1.884 \cdot Ea}. \quad (5)$$

It is known that the activation energy of the conductivity of oxides corresponds to the energy levels in the band gap created by defects in the crystal lattice. In our case, the influence of the activation energy for ZnO–SnO_2 sol–gel films appears only at an operating temperature of 250°C. As is known, at temperatures above 200–250°C, water molecules and molecules of other gases adsorbed on the oxide surface are desorbed from the surface.[25,26] At the temperature of 250°C the response of the sensor will be determined by the activation energy of conductivity.

It is known that many materials used in gas sensors of the resistive type have similar gas-sensitive characteristics. The choice of gas-sensitive materials is determined by the requirement: "simple technology — high-quality, reproducible and fast response to a given concentration". It can be seen that sensors operating at room temperature have long response/recovery times.[30–35]

Sensors with response/recovery times in the range of 30–180 s have a more complex technology for forming a gas-sensitive layer.[36–38] Some gas-sensitive materials are unstable over time, in particular metal sulfides.[38] The sol–gel method proposed in this work and in our other works[9,13,19] satisfies this requirement. Using the described method, it is possible to obtain composite nanoscale materials of various compositions with high values of gas-sensitive characteristics.

4. Conclusion

In this work, thin pore ZnO–SnO_2 films were obtained by the sol–gel method. XPS studies revealed an intense peak of plasmon losses, which suggests the reduced state of zinc in the structure of ZnO–SnO_2 sol–gel film. This state of zinc in synthesized materials can be associated with the presence of a surface electric field in thin nanocomposite films. It was confirmed by KPFM studies, which showed that the highest values of the surface potential are typical for samples of ZnO–SnO_2 sol–gel films with a Zn:Sn ratio of 1:99 and 5:95. The same samples showed high response values when exposed to nitrogen dioxide concentrations of 5–50 ppm at operating temperatures of 150°C, 200°C and 250°C. At the same time, studies have shown that at an operating temperature of 150°C, the response of a gas sensor based on ZnO–SnO_2 sol–gel depends on the value of the surface potential V_b. Moreover, the higher value of V_b corresponds to the higher

response to the nitrogen dioxide. At an operating temperature of 200°C, the value of the sensor response depends on the value of the potential barrier φ_b. However, the higher potential barrier value corresponds to the lower sensor response. Finally, at an operating temperature of 250°C, the response of the sensor will be determined by the conductivity activation energy.

Measurements of the photoconductivity kinetics of thin ZnO–SnO_2 films formed by the sol–gel method showed a change in the conductivity for all synthesized films. The response kinetics for all ZnO–SnO_2 materials was similar, which indicates the same generation mechanisms — the recombination of charge carriers in SnO_2 sol–gel films with the addition of ZnO. An estimate of the photoconductivity relaxation time constant τ showed that pure tin dioxide films have the highest value equal to 87 s. At the same time, SnO_2 films with a small addition of 0.5% ZnO have lower values of τ equal to 17 s.

Acknowledgments

The authors are grateful to the PHENMA 2021–2022 conference for the possibility of manuscript publication. The research was carried out at the expense of the grant of the Russian Science Foundation No. 22-29-00621, (https://rscf.ru/project/22-29-00621/) at the Southern Federal University. We would like to express our gratitude to the staff of the Laboratory for Technology of Functional Nanomaterials of the Institute of Nanotechnology, Electronics and Equipment Engineering of the Southern Federal University for their help in conducting SEM studies.

References

[1]E. Kowsari and M. R. Ghezelbash, Ionic liquid-assisted, facile synthesis of ZnO/SnO_2 nanocomposites, and investigation of their photocatalytic activity, *Mater. Lett.* **68**, 17 (2012).

[2]H. Uchiyama, R. Nagao and H. Kozuka, Photoelectrochemical properties of ZnO–SnO_2 films prepared by sol–gel method, *J. Alloys Compd.* **554**, 122 (2013).

[3]P. S. Huang, K. J. Lee and Y. H. Wang, Magnesium zirconate titanate thin films used as an NO_2 sensing layer for gas sensor applications developed using a sol–gel method, *Sensors* **21**, 2825 (2021).

[4]G. Williams and G. S. V. Coles, Gas sensing properties of nanocrystalline metal oxide powders produced by a laser evaporation technique, *J. Mater. Chem*. **8**, 1657 (1998).

[5]P. Gupta and V. A. Rathore, Comprehensive review: SnO_2 for photovoltaic and gas sensor applications, *Appl. Innov. Res.* (*AIR*) **1**, 184 (2020).

[6]S. Ilican, Y. Caglar, M. Caglar and F. Yakuphanoglu, Structural, optical and electrical properties of F-doped ZnO nanorod semiconductor thin films deposited by sol–gel process, *Appl. Surf. Sci.* **255**, 2353 (2008).

[7]M. Batzill and U. Diebold, The surface and materials science of tin oxide, *Progr. Surf. Sci.* **79**, 47 (2005).

[8]N. Yamazoe, J. Fuchigami, M. Kishikawa and T. Seiyama, Interactions of tin oxide surface with O_2, H_2O and H_2, *Surf. Sci.* **86**, 335 (1979).

[9]E. M. Bayan, V. V. Petrov, M. G. Volkova, V. Yu. Storozhenko and A. V. Chernyshev, SnO2–ZnO nanocomposite thin films: The influence of structure, composition and crystallinity on optical and electrophysical properties, *J. Adv. Dielect.* **11**, 2160008 (2021).

[10]M. G. Volkova, V. Yu. Storozhenko, V. V. Petrov and E. M. Bayan, Effect of tin doping on optical properties of ZnO thin films grown on glass substrate, *J. Phys.: Conf. Ser*. **1695**, 012122 (2020).

[11]R. A. Afre, N. Sharma, M. Sharon and M. Sharon, Transparent conducting oxide films for various applications: A review, *Rev. Adv. Mater. Sci.* **53**, 79 (2018).

[12]J. Sheng, K. L. Han, T. Hong, W. H. Choi and J. S. Park, Review of recent progresses on flexible oxide semiconductor thin film transistors based on atomic layer deposition processes, *J. Semicond.* **39**, 011008 (2018).

[13]V. V. Petrov, V. V. Sysoev, A. P. Starnikova, M. G. Volkova, Z. K. Kalazhokov, V. Yu. Storozhenko, S. A. Khubezhov and E. M. Bayan, Synthesis, characterization and gas sensing study of ZnO–SnO_2 nanocomposite thin films, *Chemosensors* **9**, 124 (2021).

[14]L. Sen, Zh. Yaqing, G. Shang, F. Teng, Zh. Yong, Zh. Xuejun and Zh. Tong, An organometallic chemistry-assisted strategy for modification of zinc oxide nanoparticles by tin oxide nanoparticles: Formation of *n-n* heterojunction and boosting NO_2 sensing properties, *J. Colloid Interface Sci.* **567**, 328 (2020).

[15]V. V. Petrov, N. K. Plugotarenco, N. T. Nazarova and A. N. Korolev, Preparation of sols from water–alcohol solutions of tetraethyl orthosilicate and $SnCl_4$ and the effect of sol composition on the surface morphology of sol–gel films, *Inorg. Mater.* **43**, 1010 (2007).

[16]V. A. Shmatko, G. E. Yalovega, T. N. Myasoedova, M. M. Brzhezinskaya, I. E. Shtekhin and V. V. Petrov, Influence of the surface morphology and structure on the gas-sorption properties of SiO_2CuO × nanocomposite materials: X-ray spectroscopy investigations, *Phys. Solid State* **57**, 399 (2015).

[17]R. K. Sonker, A. Sharma, M. Tomar, V. Gupta and B. C. Yadav, Low temperature sensing of NO2 gas using SnO2–ZnO nanocomposite sensor, *Adv. Mat. Lett.* **4**, 196 (2013).

[18]B.Yea, R. Konishi, T. Osaki, S. Abe, H. Tanioka and K. Sugahara, Analysis of the sensing mechanism of tin dioxide thin film gas sensors using the change of work function in flammable gas atmosphere, *Appl. Surf. Sci.* **100/101**, 365 (1996).

[19]A. P. Starnikova, I. A. Gulyaeva, V. Yu. Storozhenko, M. G. Volkova, E. M. Bayan and V. V. Petrov, Study of the electrophysical and gas-sensitive properties of thin ZnO–SnO2 films formed by the sol–gel method, *J. Phys.: Conf. Ser.* **2103**, 012132 (2021).

[20]A. P. Starnikova, A. V. Nesterenko, A. V. Petrov, Yu. N. Varzarev and V. V. Petrov, Research of the photoconductivity characteristics of thin films of complex oxides formed on non-transparent substrates, *Physics of Lead-free Piezoactive and Related Materials. Modeling of Eco-systems. Proc 10th Int. Symp.* (2021), pp. 125–126.

[21]E. C. Onyiriuka, Zinc phosphate glass surfaces studied by XPS, *J. Non-Cryst. Solids* **163**, 268 (1993).

[22]N. Benito, G. Recio-Sánchez, R. Escobar-Galindo and C. Palacio, Formation of antireflection Zn/ZnO core–shell nano-pyramidal arrays by O_{2+} ion bombardment of Zn surfaces, *Nanoscale* **9**, 14201 (2017).

[23]M. Kwoka and M. Krzywiecki, Impact of air exposure and annealing on the chemical and electronic properties of the surface of SnO2 nanolayers deposited by rheotaxial growth and vacuum oxidation, *Beilstein J. Nanotechnol.* **8**, 514 (2017).

[24]I. A. Averin, A. A. Karmanov, V. A. Moshnikov, R. M. Pecherskaya and I. A. Pronin, Features of synthesis and research of nanocomposite films produced sol–gel technology method, *University proceedings. Volga region. Physical and mathematical sciences* **2** (2012) (in Russian).

[25]V. A. Moshnikov, I. E. Gracheva, V. V. Kuznezov, A. I. Maximov, S. S. Karpova and A. A. Ponomareva, Hierarchical nanostructured semiconductor porous materials for gas sensors, *J. Non-Cryst. Solids* **356** 2020 (2010) (in Russian) – page no. 2020.

[26]A. I. Maksimov, V. A. Moshnikov, Yu. M. Tairov and O. A. Shilova, Basics of sol–gel technology of nanocomposites, *St. Petersburg: Elmor,* 2nd edn. (2008) (in Russian).

[27]K. V. Shalimova, *Semiconductor Physics*, 2nd edn. Moscow: Energy, 1976.

[28]E. Comini, V. Guidi, C. Malagu, G. Martinelli, Z. Pan, G. Sberveglieri and Z. L. Wang, Electrical properties of tin dioxide two-dimensional nanostructures, *J. Phys. Chem. B* **108**, 1882 (2004).

[29]G. F. McAller, P. T. Moseley, J. O. W. Norris and D. E. Williams, Tin dioxide gas sensors. Part 1 — Aspects of the surface chemistry revealed by electrical conductance variations, *J. Chem. Soc. Faraday Trans*. **83**, 1323 (1987).

[30]M. Popescu, I. D. Simandan, F. Sava, A. Velea and E. Fagadar-Cosma, Sensor of nitrogen dioxide based on single wall carbon nanotubes and manganese-porphyrin, *Biostruct.* **6** 1253 (2011) – page no.1253.

[31]D. Matatagui, C. Cruz, F. Carrascoso, A. M. Al-Enizi, A. Nafady, A. Castellanos-Gomez and M. d. C. Horrillo, Eco-friendly disposable WS_2 paper sensor for sub-ppm NO_2 detection at room temperature, *Nanomaterials* **12**, 1213 (2022).

[32]S. Goutham, K. K. Sadasivuni, D. S. Kumarc and K. V. Rao, Flexible ultra-sensitive and resistive NO_2 gas sensor based on nanostructured $Zn_{(x)}Fe_{(1-\ x)2}O_4$, *RSC Adv.* **8** 3243 (2018) – page no. 3243.

[33]T. Ueda, I. Boehme, T. Hyodo, Y. Shimizu, U. Weimar and N. Barsan, Effects of gas adsorption properties of an Au-loaded porous In_2O_3 sensor on NO_2-sensing properties, *ACS Sens.* **6** 4019 (2021) – page no. 4019.

[34]V. Kampitakis, E. Gagaoudakis, D. Zappa, E. Comini, E. Aperathitis, A. Kostopoulos, G. Kiriakidis and V. Binas, Highly sensitive and selective NO_2 chemical sensors based on Al doped NiO thin films, *Mater. Sci. Semicond. Process.* **115***,* 105149 (2020).

[35]C. C. Hewa-Rahinduwage, X. Geng, K. L. Silva, X. Niu, L. Zhang, S. L. Brock and L. Luo, Reversible electrochemical gelation of metal chalcogenide quantum dots, *J. Am. Chem. Soc.* **142** 12207 (2020) – page no. 12207.

[36]J. Zhang, D. Leng, L. Zhang, G. Li, F. Ma, J. Gao, H. Lu and B. Zhu, Porosity and oxygen vacancy engineering of mesoporous WO_3 nanofibers for fast and sensitive low-temperature NO_2 sensing, *J. Alloys Compd.* **853**, 157339 (2021).

[37]W. Zeng, Y. Liu, G. Chen, H. Zhan, J. Mei, N. Luo, Z. He and C. Tang, SnO–Sn_3O_4 heterostructural gas sensor with high response and selectivity to parts-per-billion-level NO_2 at low operating temperature, *RSC Adv.* **10** 29843 (2020) – page no. 29843.

[38]Z. Li, H. Li, Z. Wu, M. Wang, J. Luo, H. Torun, P. Hu, C. Yang, M. Grundmann, X. Liu and Y. Q. Fu, Advances in designs and mechanisms of semiconducting metal oxide nanostructures for high-precision gas sensors operated at room temperature, *Mater. Horiz.* **6** 470 (2019) – page no. 470.